ANNALS of Clinical and Translational Neurology
Open Access
ANA American Neurological Association since 1875

RESEARCH ARTICLE

# Diazepam effect during early neonatal development correlates with neuronal $Cl^-$

Joseph Glykys[1,2] & Kevin J. Staley[1,2]

[1]Department of Neurology, Massachusetts General Hospital, Boston, Massachusetts
[2]Harvard Medical School, Boston, Massachusetts

**Correspondence**
Joseph Glykys, Department of Neurology. Massachusetts General Hospital, Boston, MA. Tel: 617-726-6833; Fax: 617-643-0141; E-mail: jglykys@mgh.harvard.edu

**Funding Information**
This work was supported by the American Academy of Neurology/the American Brain Foundation/Beyond Batten Disease Foundation Fellowship and the National Institute of Neurological Disorders and Stroke/NIH (Grant : 5R01NS40109-14, R01NS74772-04).

Received: 11 September 2015; Accepted: 16 September 2015

***Annals of Clinical and Translational Neurology*** **2015; 2(12): 1055–1070**

doi: 10.1002/acn3.259

## Abstract

**Objective**: Although benzodiazepines and other $GABA_A$ receptors allosteric modulators are used to treat neonatal seizures, their efficacy may derive from actions on subcortical structures. Side effects of benzodiazepines in nonseizing human neonates include myoclonus, seizures, and abnormal movements. Excitatory actions of GABA may underlie both side effects and reduced anticonvulsant activity of benzodiazepines. Neocortical organotypic slice cultures were used to study: (1) spontaneous cortical epileptiform activity during early development; (2) developmental changes in $[Cl^-]_i$ and (3) whether diazepam's anticonvulsant effect correlated with neuronal $[Cl^-]_i$. **Methods**: Epileptiform activity in neocortical organotypic slice cultures was measured by field potential recordings. $Cl^-$ changes during development were assessed by multiphoton imaging of neurons transgenically expressing a Cl-sensitive fluorophore. Clinically relevant concentrations of diazepam were used to test the anticonvulsant effectiveness at ages corresponding to premature neonates through early infancy. **Results**: (1) Neocortical organotypic slices at days in vitro 5 (DIV5) exhibited spontaneous epileptiform activity. (2) Epileptiform event duration decreased with age. (3) There was a progressive decrease in $[Cl^-]_i$ over the same age range. (4) Diazepam was ineffective in decreasing epileptiform activity at DIV5-6, but progressively more effective at older ages through DIV15. (5) At DIV5-6, diazepam worsened epileptiform activity in 50% of the slices. **Interpretation**: The neocortical organotypic slice is a useful model to study spontaneous epileptiform activity. Decreasing $[Cl^-]_i$ during development correlates with decreasing duration of spontaneous epileptiform activity and increasing anticonvulsant efficacy of diazepam. We provide a potential explanation for the reports of seizures and myoclonus induction by benzodiazepines in newborn human neonates and the limited electrographic efficacy of benzodiazepines for the treatment of neonatal seizures.

## Introduction

GABA binding to $GABA_A$ receptors ($GABA_AR$) allows the flux of $Cl^-$ and to a lesser extent bicarbonate based on their concentration gradients. The intracellular chloride concentration ($[Cl^-]_i$) mainly determines the reversal potential of GABA ($E_{GABA}$) as $Cl^-$ has five times the permeability of bicarbonate.[1] The relation between $E_{GABA}$ and the resting membrane potential (RMP) of a neuron determines if GABA actions are excitatory ($E_{GABA}$ significantly above RMP) or inhibitory ($E_{GABA}$ near or below RMP).[2–4] Early during neonatal development, neuronal $[Cl^-]_i$ is elevated, leading to GABA-gated $Cl^-$ efflux and GABA-mediated excitation. During maturation, the neuronal $[Cl^-]_i$ progressively decreases making GABA actions inhibitory.[5–9]

The neocortex shows the most delayed development in neuronal $[Cl^-]_i$ compared to other brain regions.[6,10,11] This gradual development of a lower $[Cl^-]_i$ was initially thought to result mainly due to a differential expression of $Cl^-$ co-transporters (CCC).[11–14] However, recent evidence indicates that negatively charged extracellular and

intracellular macromolecules[15,16] displace $Cl^-$ and thus determine the $[Cl^-]_i$, in which case, developmental and activity-dependent increases in these macromolecules[17,18] would drive the reduction in $[Cl^-]_i$.[19,20] CCCs serve to maintain this distribution in the face of synaptic $Cl^-$ flux.[19–22] The many studies of developmental changes in GABA signaling have raised questions regarding the current practice of using GABAergic anticonvulsants to treat neonatal seizures.[23]

Human neonatal seizures are difficult to treat. Phenobarbital and phenytoin, the most common first line agents, have poor effectiveness in this age group.[24–26] In mice, phenobarbital's poor effectiveness in the neocortex is correlated with the developmentally high $[Cl^-]_i$ while thalamic neurons, which have a low $[Cl^-]_i$ during early development, respond well to this drug.[6] Benzodiazepines are more selective $GABA_AR$ positive allosteric modulators frequently used to treat refractory human neonatal seizures.[24,27,28] However, they also show decreased effectiveness in this age group.[29–31] Interestingly, in some premature and full term human neonates, benzodiazepines can actually induce seizures, myoclonus, and abnormal movements.[32–36] These data suggest that neuronal $[Cl^-]_i$ may alter the anticonvulsant effectiveness of benzodiazepines in neonates.

Hippocampal organotypic slices develop spontaneous seizures after a short silent period.[37–40] They can be used to study anticonvulsive medications without applying convulsant conditions such as altered $Mg^{2+}$ [41,42] and $K^+$ concentration,[43,44] blocking $K^+$ channels with 4-aminopyridine,[45,46] or activating kainate receptors.[47] However, the neocortex is compromised much more commonly than the hippocampus in the neonatal period.[48] We therefore investigated whether isolated neocortical organotypic slice cultures, devoid of modulatory subcortical connections, could also comprise a useful model to study neonatal seizures and epileptogenesis. However, it remains unknown whether spontaneous epileptiform activity develops in this preparation as it does in the hippocampal slice cultures.

Therefore, we studied: (1) if the disconnected neocortical organotypic slice cultures develop spontaneous epileptiform activity; (2) if neuronal $[Cl^-]_i$ changes with age as seen in acute brain slices and finally, (3) if benzodiazepine effects on epileptiform activity are correlated with the neuronal $[Cl^-]_i$ in this preparation.

## Methods

### Organotypic slice culture

All animal protocols were approved by the Massachusetts General Hospital Center for Comparative Medicine. Neocortical slices were prepared at postnatal day 6–7 from C57BL/6 mice (The Jackson Laboratory, Bar Harbor, ME) and from Clomeleon mice. Clomeleon mice express a genetically encoded $Cl^-$ ratiometric fluorophore.[49] Slice cultures were prepared as described for hippocampal organotypic cultures.[37,50] Briefly, coronal 400-$\mu$m-thick neocortical slices (frontal region, prehippocampus) were cut using a McIlwain tissue chopper (Mickle Laboratory Eng. Co., Surrey, U. K.; Fig. 1A). Slices were mounted in clots of chicken plasma (Cocalico Biologicals, Reamstown, PA) and thrombin on poly-L-lysine-coated glass coverslips (Sigma-Aldrich, St. Louis, MO). Slices were incubated in roller tubes (Nunc, Roskilde, Denmark) at 36°C with 750 $\mu$L of Neurobasal A/B27 medium supplemented with 0.5 mM GlutaMAX, 30 $\mu$g/mL gentamicin (Life Technologies, Grand Island, NY) and 20 mM NaCl to reach a final media osmolarity of 280 $\pm$ 5 mOsm (mean $\pm$ SD, $n = 7$). The culture media were changed biweekly.

### Electrophysiology recordings

Organotypic neocortical slices were placed in a conventional submerged chamber and continuously perfused with oxygenated artificial cerebrospinal fluid (aCSF) (95% $O_2$–5% $CO_2$) at 32–34°C with a flow rate of 5–8 mL/min. aCSF contained the following compounds (mM): NaCl (120), KCl (3.3), $CaCl_2$ (1.3), $MgCl_2$ (1.3), $NaH_2PO_4$ (1.25), $NaHCO_3$ (25), and D-glucose (11) with pH 7.3–7.4 when bubbled with 95% $O_2$ and 5% $CO_2$. Extracellular field potential recordings in neocortical layer II/III were performed using tungsten microelectrodes and a low-noise multichannel amplifier (Dagan EX 4-400) with a 1000 gain and digitized at 2 kHz using an analog to digital converter DigiData 1321A (Molecular Devices, Sunnyvale, CA.).

**Figure 1.** Decrease in $[Cl^-]_i$ during early development in neocortical organotypic slices. (A) Micrographs of neocortical organotypic slices kept at DIV5 (*left*), DIV9 (*middle*) and DIV15 (*right*). Scale bar 1 mm. 2× magnification, bright-field image. (B) Two-photon images of Clomeleon in neocortical organotypic slices at DIV6 (*left*), DIV9 (*middle*) and DIV15 (*right*). Overlay of multiple *z*-planes. *Top panels*, YFP; *lower panels*, neuronal $Cl^-$ pseudocolored based on YFP/CFP ratio. (C) Probability density distribution of neuronal $[Cl^-]_i$ at the different ages. (D) Percentage distribution of neurons with different binned $[Cl^-]_i$. Same colors as in (B). (E) $[Cl^-]_i$ median $\pm$ SD at different ages ($P < 0.001$, One-way ANOVA on Ranks. *$P < 0.005$, Dunn's method). (F) $[Cl^-]_i$ as a function of depth for all neurons. DIV6: slope = −0.07 mM/$\mu$m, $R = -0.13$, $P = 0.006$; DIV9–10: slope = −0.02 mM/$\mu$m, $R = -0.10$, $P = 0.003$; DIV15–16: slope = −0.06 mM/$\mu$m, $R = -0.22$, $P < 0.001$. DIV, days in vitro; ANOVA, analysis of variance.

 

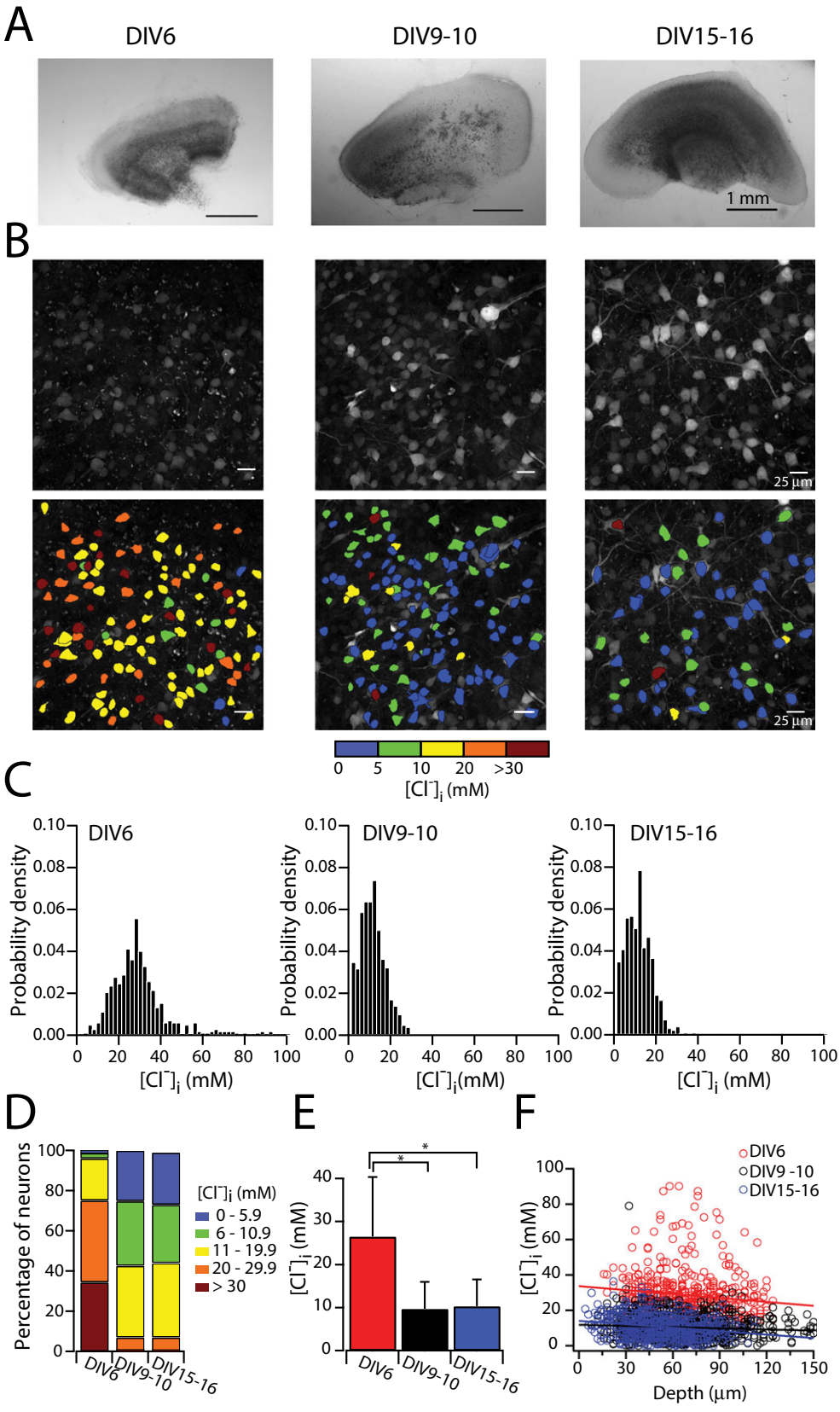


 

## Electrophysiological analysis

### FFT area

Analysis was performed using a custom-written macro running under IGOR Pro v6.35 (Lake Oswego, OR) as previously described.[6] Briefly, the complete trace was loaded. For each 30 sec epoch, its mean value was subtracted and Fast Fourier Transformed (FFT) using a Hanning window apodization. Next, the FFT was smoothed with a median window of seven points, divided by the total number of points, and the signal area (1–500 Hz) was calculated (FFT power). The wide-band power is equal to the square of the field potential, and thus represents an unbiased measure to quantify seizure activity. Finally, the mean FFT power during equal control and drug condition epochs was calculated.

### Epileptiform characteristics

The duration and interevent interval of the epileptiform discharges were measured with DClamp v3.5, a custom and freely available data acquisition and analysis software (https://sites.google.com/site/dclampsoftware/home). All events were visually inspected. The epileptiform activity burden was calculated by dividing the total duration of epileptiform activity by the total time during the same time window used to calculate the FFT power.

## $Cl^-$ imaging and analysis

Two-photon fluorescence imaging of neurons expressing Clomeleon was obtained using a Fluoview 1000MPE with prechirp optics and a fast acousto-optical modulator mounted on a Olympus BX61WI upright microscope (Olympus Corporation, Tokyo, Japan) using a 20× water immersion objective (NA 0.95). A mode-locked Ti:Sapphire laser (MaiTai, Spectra Physics, Fermont, CA) generated two-photon fluorescence with 860 nm excitation. Emitted light passed through a dichroic mirror (460 nm cutoff) and was band-pass filtered through 480 ± 15 nm filter (D480/30) for cyan fluorescent protein (CFP) and 535 ± 20 nm filter (D535/40) for yellow fluorescent protein (YFP). Two photomultiplier tubes (Hamamatsu Photonics, Hamamatsu City, Japan ) were used to simultaneously acquire CFP and YFP signals. Three-dimensional stacks (3D) of raster scans in the XY plane were imaged at $z$-axis intervals of 1–2 $\mu$m. Clomeleon-expressing neurons were imaged in the neocortex in slices perfused with aCSF + 1 μM tetrodotoxin (TTX; selective inhibitor of $Na^+$ channels) to prevent spontaneous epileptiform activity, held at 32–34°C and aerated with 95% $O_2$–5% $CO_2$. ImageJ 1.47 software (NIH, Bethesda, MD) was used for quantitative analysis.

### $[Cl^-]_i$ determination

Neuronal $[Cl^-]_i$ measurement was performed as described before.[6,19] Briefly, the CFP and YFP respective background values were subtracted from each XY plane. Next, a median filter was applied to all of the XY images. A region of interest (ROI) was drawn around the neurons bodies and the mean ratio of the YFP/CFP fluorescence intensity was calculated for each pixel in the ROI. Each cell's YFP/CFP mean ratio was converted into $Cl^-$ value by the following equation:

$$[Cl^-]_i = K'_D \frac{(R_{max} - R)}{(R - R_{min})}$$

$K'_D$ is the apparent dissociation constant, $R_{max}$ is the ratio when no Clomeleon is bound by $Cl^-$, and $R_{min}$ is the ratio when Clomeleon is completely quenched.[49] The median $[Cl^-]_i$ was used as the distribution of $[Cl^-]_i$ in neurons is skewed to lower values. Occasional neurons whose ratio was outside the calibration curve were excluded.

## Statistical analysis

$[Cl^-]_i$ was expressed as a median ± SD as $[Cl^-]_i$ follows a non-Gaussian distribution. One-way analysis of variance (ANOVA) on ranks with post hoc Dunn's method was used for multiple comparisons of nonparametric data. One-way ANOVA with post hoc Holm–Sidak test was used for multiple comparisons of parametric data. The Wilcoxon Signed Rank Test was used for nonparametric paired data. Paired $t$-tests were used for parametric paired comparisons. Chi-square was used when comparing proportions. Statistical significance was set to $P < 0.05$. Igor Pro and SigmaPlot v11 (Systat Software, Inc, San Jose, CA) were used for data analysis.

## Reagents

TTX was obtained from Tocris. Diazepam (Sigma-Aldrich) was dissolved in 100% ethanol (final concentration of ethanol in solution 0.000005%). Equal volume of ethanol, as used in the diazepam solution, was added to the control solution.

# Results

## Neocortical $[Cl^-]_i$ decreases during early development

$[Cl^-]_i$ decreases during early development in different brain areas.[5,10] Neocortical acute slices show a progressive

 

decrease in $[Cl^-]_i$ during early development[6] which correlates with more negative $E_{GABA}$ values.[2,4,51] In acute hippocampal slices, the most superficial areas show high neuronal $[Cl^-]_i$ values due to slicing trauma.[52] To remove acute trauma as a variable, we studied $[Cl^-]_i$ in neocortical organotypic slice cultures (frontal region, pre-hippocampus) from Clomeleon mice prepared at P6–7. Clomeleon is a genetically encoded ratiometric fluorophore sensitive to $[Cl^-]_i$.[49] We measured $[Cl^-]_i$ using multiphoton microscopy starting 6 days after slice preparation (DIV6, days in vitro), at DIV9–10 and at DIV15–16. Hundreds of neurons can be imaged with fluorescence microscopy simultaneously as compared to other $[Cl^-]_i$ measuring techniques. Layer IV/V neurons were imaged (from surface to the depth of the slice) in regular aCSF + 1 μM TTX (selective inhibitor of $Na^+$ channels) to avoid spontaneous epileptiform activity that can cause $Cl^-$ accumulation.[53] $[Cl^-]_i$ decreased during early development in layer IV/V neocortical neurons from organotypic slices on a time scale that was similar to acute neocortical slices.[6] At DIV6, $[Cl^-]_i$ was 26.6 ± 13.8 mM (median ± SD, $n$ = 482 neurons, six slices, two animals, range 4–90 mM) and showed a wide distribution (Fig. 1B and C). In comparison, $[Cl^-]_i$ dropped to 9.7 ± 6.3 mM

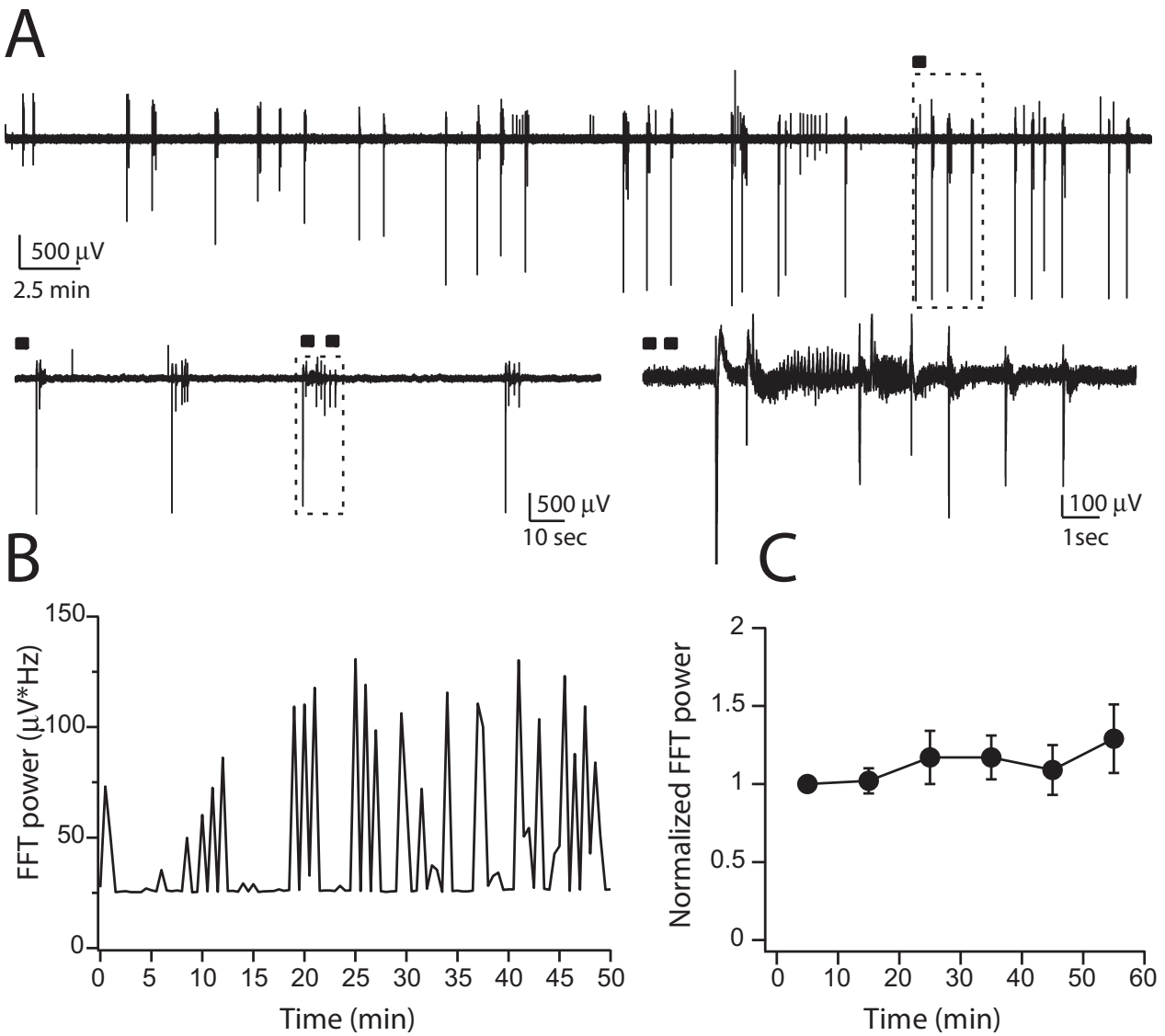


**Figure 2.** Stability of epileptiform activity in neocortical organotypic slices. (A) *Upper panel:* Extracellular recording showing stable epileptiform activity recorded in regular aCSF from layer II/III of a DIV7 organotypic neocortical slice. *Lower panel, left:* ■ magnified events from dashed box in upper panel. *Right:* ■ ■ magnified event from dashed box in left panel. (B) FFT power calculated every 30 sec from the trace in (A). (C) Normalized FFT power to the first initial 10 min in each recording (DIV5–7, $n$ = 6). DIV, days in vitro; FFT, Fast Fourier Transform.

 

at DIV9–10 ($n = 984$ neurons, 10 slices, two animals, range 0–79; Fig. 1B and C) with no significant further change by DIV 15–16 (10.3 ± 6.2 mM; $n = 597$ neurons, 11 slices, two animals, range 0–36; Fig. 1B and C). At DIV6, 75% of neurons had $[Cl^-]_i$ above 20 mM compared to 7% at DIV9–10 or DIV15–16 (Fig. 1D). The $[Cl^-]_i$ was significantly different between the different ages (One-way ANOVA on Ranks, $P < 0.001$) and specifically between DIV6 and both DIV9–10 and DIV15–16 (Dunn's method, $P < 0.005$; Fig. 1E).

Acute hippocampal slices demonstrated that the $[Cl^-]_i$ depends on the depth of the neuron imaged, where the most superficial neurons have higher $[Cl^-]_i$ than deeper ones.[52] In contrast, the neocortical organotypic slice $[Cl^-]_i$ showed a small linear relationship with depth at all ages tested (range: −0.02 to −0.07 mM/$\mu$m; Fig. 1F). The current results confirm the developmental decrease in $[Cl^-]_i$ during early development initially observed in acute neocortical slices,[6] and which is independent from slice trauma. Next, we tested whether the neocortical organotypic slices have spontaneous epileptiform activity.

## Neocortical organotypic slices show spontaneous epileptiform activity

Hippocampal organotypic slices show spontaneous interictal activity, as well as ictal activity starting at DIV7.[37,38,40] The minimal duration of an epileptiform activity to be classified as a seizure, in an in vitro model ranges from 0.8 to 10 sec.[54–56] Therefore, we decided to call all abnormally synchronous activity "epileptiform" to encompass interictal and ictal events, and events >10 sec were defined as ictal. Epileptiform activity was quantified by the FFT power every 30 sec as previously described[19] (see Methods, Fig. 2B). The wide-band power is proportionately affected by the frequency of discharge, its synchrony, the duration of the discharge, and the fraction of the neuronal population participating in the discharge. This method allowed us to have an integral of the frequency, duration, and amplitude of the events during the whole recording.

Field potential recordings were obtained from layer II/III of the neocortical organotypic slices derived from C57Bl6 mice which showed spontaneous epileptiform activity in regular aCSF starting at DIV5 (Fig. 2A and B). In these set of experiments, 100% of DIV5 neocortical organotypic slices showed epileptiform activity that was stable over time (Fig. 2C). Therefore, this preparation was suitable to study spontaneous epileptiform activity during early development, its relation with $[Cl^-]_i$ and its response to a clinically relevant diazepam dose.

## Epileptiform activity changes during early development

Spontaneous epileptiform activity in neocortical organotypic slices (layer II/III; frontal region, pre-hippocampus) was recorded at three different developmental ages in regular aCSF: DIV5–6, DIV9–10 and DIV15. All ages showed epileptiform activity.

Epileptiform event duration decreased as the slices matured (one-way ANOVA on Ranks, $P < 0.001$; specifically between DIV5–6 and DIV15–16 and between DIV9–10 and DIV15–16, Dunn's Method, $P < 0.05$; Table 1). The percentage of ictal events (events lasting more than 10 sec) was also different between ages ($\chi^2$, $P < 0.001$; Table 1). The interevent interval of the epileptiform events decreased as the slices matured (one-way ANOVA on Ranks, $P < 0.001$; difference between all ages, Dunn's method, $P < 0.05$; Table 1). The epileptiform activity burden (the proportion of time a slice is having epileptiform activity) is another measurement parameter that combines the event duration and the interevent interval. This burden was increased during in vitro development (one-way ANOVA, $P < 0.001$, Holm–Sidak post hoc test showed differences between all the different ages, $P < 0.05$; Table 1).

These data indicate that as slices mature and $[Cl^-]_i$ decreases, the duration of epileptiform events decreases, the frequency of the events increases and the proportion of time generating epileptiform activity increases from 5% to 22%. We next wanted to determine if a clinically meaningful diazepam dose would have a larger effect at older developmental ages at which more neurons have a $[Cl^-]_i$ in the range that renders $GABA_AR$ activation strictly inhibitory.

## Diazepam effect is dependent on $[Cl^-]_i$

Diazepam is a $GABA_AR$ positive allosteric modulator that increases the channel current by increasing the frequency of channel openings.[57–59] We reasoned that if $[Cl^-]_i$ is higher during early development, a clinically relevant concentration of diazepam should be ineffective or even potentiate the epileptiform activity. The high $[Cl^-]_i$ in many neurons would favor a depolarizing efflux of $Cl^-$ based on the relation of $E_{Cl}$ and the RMP. In contrast, at older developmental ages, when $[Cl^-]_i$ is lower in the majority of neurons, diazepam should exert a net enhancement of inhibition in the network. Drug plasma concentrations of 0.15 mg/L [range: 0.07–0.23 mg/L] can be found in human neonates after receiving diazepam at anticonvulsant doses (0.1–0.3 mg/kg with a volume of distribution of 1.3 L/kg).[60,61] We used a clinical relevant

 

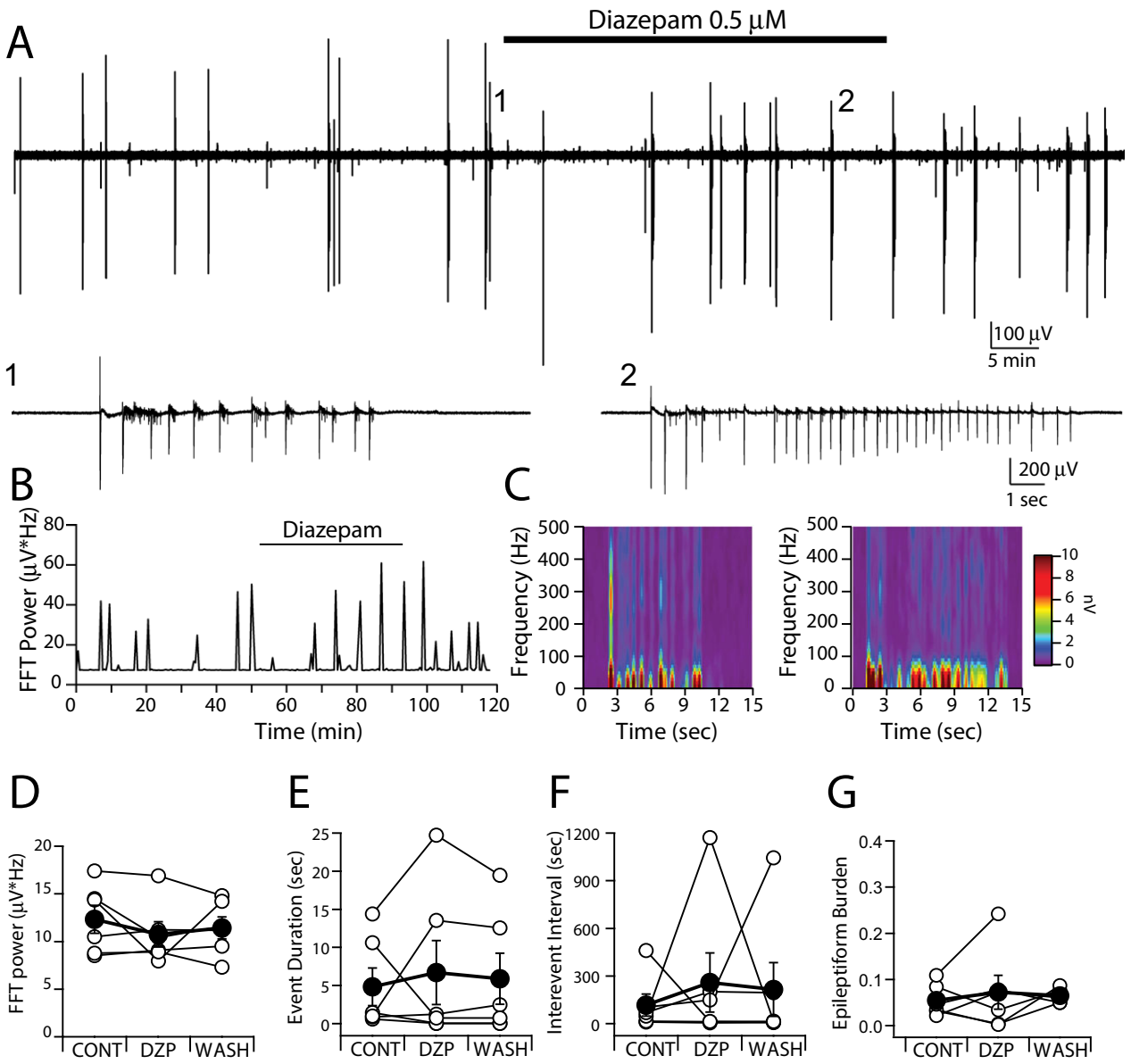


**Figure 3.** Diazepam is ineffective in decreasing epileptiform activity at DIV5–6 in neocortical organotypic slices. (A) Extracellular recording of epileptiform activity recorded in regular aCSF from layer II/III of a DIV5 organotypic neocortical slice. Diazepam perfusion indicated with black line. Lower panels are higher magnifications of characteristic events in control condition (1) and during diazepam perfusion (2). (B) FFT power calculated every 30 sec from the trace in (A), showing a 7% increase in FFT during diazepam perfusion in this slice. (C) FFT power calculated every 500 msec for the events numbered 1 and 2 in (A). (D) FFT power showing no significant difference between paired control (CONT), diazepam (DZP) and washout (WASH) conditions. (E) Event duration between the three conditions. (F) Interevent interval between the three conditions. (G) Epileptiform burden between the three conditions. Note that in all the forms of measurement there is dichotomy. Dark circles are mean ± SEM; $n = 6$. DIV, days in vitro; FFT, Fast Fourier Transform.

dose of 0.5 μM of diazepam, corresponding to 0.14 mg/L, to test our hypothesis.

First, epileptiform activity was measured by obtaining the FFT power every 30 sec from the neocortical organotypic slice layer II/III recorded in regular aCSF. Matched time windows were used to compare the diazepam effect to control conditions. Diazepam (0.5 μM) produced a nonsignificant 10% decrease in the epileptiform FFT power at DIV5–6 (one-way repeated measures ANOVA, $P = 0.365$; $n = 6$; Figs. 3A–D, 6A; Table 2). This drug concentration also did not change the event duration (one-way repeated measures ANOVA, $P = 0.773$; Figs. 3E,

 

**Table 1.** Epileptiform activity characteristics of neocortical organotypic slices during different in vitro ages.

| | Event duration (sec) | Ictal events (%) | Interevent interval (sec) | Epileptiform activity burden | *N* (events) | *N* (slices) |
|---|---|---|---|---|---|---|
| DIV5–6 | 2.57 ± 0.26 | 8.55 | 54.3 ± 6.42 | 0.05 ± 0.01 | 269 | 6 |
| DIV9–10 | 1.70 ± 0.08 | 3.01 | 11.4 ± 0.77 | 0.15 ± 0.01 | 1294 | 7 |
| DIV15–16 | 1.16 ± 0.04 | 0.79 | 4.98 ± 0.13 | 0.22 ± 0.03 | 2406 | 6 |
| *P* value | <0.001 | <0.001[1] | <0.001 | <0.001 | | |

Ictal events: events lasting >10 sec. Mean ± SEM. One-way ANOVA *P* values. DIV, days in vitro; ANOVA, analysis of variance.
[1]Chi-square *P* value. See text for further details.

6B; Table 2), interevent interval (repeated measures ANOVA on ranks, $P = 0.740$; Figs. 3F, 6C; Table 2) or epileptiform activity burden (one-way repeated measures ANOVA, $P = 0.442$; Figs. 3G, 6D; Table 2). Three of six slices responded with an increase in all measures in the presence of diazepam while 3/6 responded with a decrease. This suggests that at this age diazepam can be either pro or anticonvulsant.

Diazepam 0.5 μM had an anticonvulsant effect at older ages. At DIV9–10 there was a 21% decrease in epileptiform FFT power (paired *t*-test, $P = 0.041$; $n = 7$; Figs. 4A-D, 6A). There was no significant decrease in event duration (paired *t*-test, $P = 0.135$) or in interevent interval (Wilcoxon Signed Rank test, $P = 0.297$; Fig. 4E and F; Table 2). However, and similar to the FFT power, the epileptiform activity burden was significantly reduced (paired *t*-test, $P = 0.041$; Fig. 4G and 6D; Table 2). This suggests that the measurements of FFT power and epileptiform activity burden are more sensitive in finding drug effects than event duration and interevent interval alone. In comparison to DIV5–6, only 1/7 slices increased the event duration and 3/7 decreased the interevent interval (Fig. 6B and C). This suggests that at this age, diazepam exerted a net anticonvulsant effect on most neocortical networks.

The anticonvulsant effect of 0.5 μM diazepam was more robust at DIV15–16. There was a 41% decrease in epileptiform FFT power at this age (paired *t*-test, $P = 0.009$; $n = 6$; Figs. 5A-D, 6A; Table 2). There was a significant decrease in event duration (paired *t*-test, $P = 0.012$) but not in the interevent interval (Wilcoxon Signed Rank test, $P = 0.438$; Figs. 5E and F, 6B and C; Table 2). Similar to the FFT power, the epileptiform activity burden decreased significantly (paired *t*-test, $P < 0.001$; Figs. 5G, 6D; Table 2). At this age 0/6 slices increased the event duration and 2/6 decreased the interevent interval in the presence of diazepam (Fig. 6B and C). These results suggest that diazepam is a more effective anticonvulsant medication at this older age.

Finally, a one-way ANOVA of the effect of diazepam (decreasing the FFT power) as a function of age was statistically significant (one-way ANOVA, $P = 0.027$) and specifically between DIV5–6 and DIV15–16 (Holm–Sidak method, $P = 0.009$; Fig. 6A). In conclusion, a clinically relevant dose of diazepam will have a differential effect (pro or anticonvulsant) based on the baseline $[Cl^-]_i$.

## Discussion

We conclude the following: (1) Organotypic neocortical slices develop spontaneous epileptiform activity by DIV5. (2) DIV15–16 slices generate a higher proportion of interictal like activity versus ictal events. (3) Diazepam, at a clinically relevant dose, is not an effective anticonvulsant at early ages. (4) The more effective anticonvulsant effect of diazepam at older ages correlates with lower $[Cl^-]_i$. We conclude that our data provide an explanation for the limited anticonvulsant efficacy of benzodiazepines, as well as the occasional ictogenic side effects in neonates and particularly premature infants.

Organotypic neocortical slice cultures at DIV5 and older develop spontaneous epileptiform activity in regular aCSF with 1.3 mM $MgCl_2$. To our knowledge, this is the first report of spontaneous epileptiform activity in this brain region with regular aCSF. This is similar to what

**Figure 4.** Diazepam is effective in decreasing epileptiform activity at DIV9–10 neocortical organotypic slices. (A) Extracellular recording of epileptiform activity recorded in regular aCSF from layer II/III of a DIV9 organotypic neocortical slice. Diazepam perfusion indicated with black line. (B) *Upper panels:* Higher magnification of characteristic events from dashed boxes in (A). Control condition (1), diazepam condition (2). *Lower panels:* higher magnifications of events in dashed boxes from upper panels. Control condition (■), diazepam condition (●). (C) FFT power calculated every 30 sec from the trace in (A). (D) FFT power was statistically different between paired control (CONT) and diazepam (DZP) conditions. (E) Event duration between paired conditions. (F) Interevent interval between paired conditions. (G) Epileptiform burden was statistically different between paired conditions. Dark circles are mean ± SEM; $n = 7$; paired *t*-test. DIV, days in vitro; FFT, Fast Fourier Transform.

 

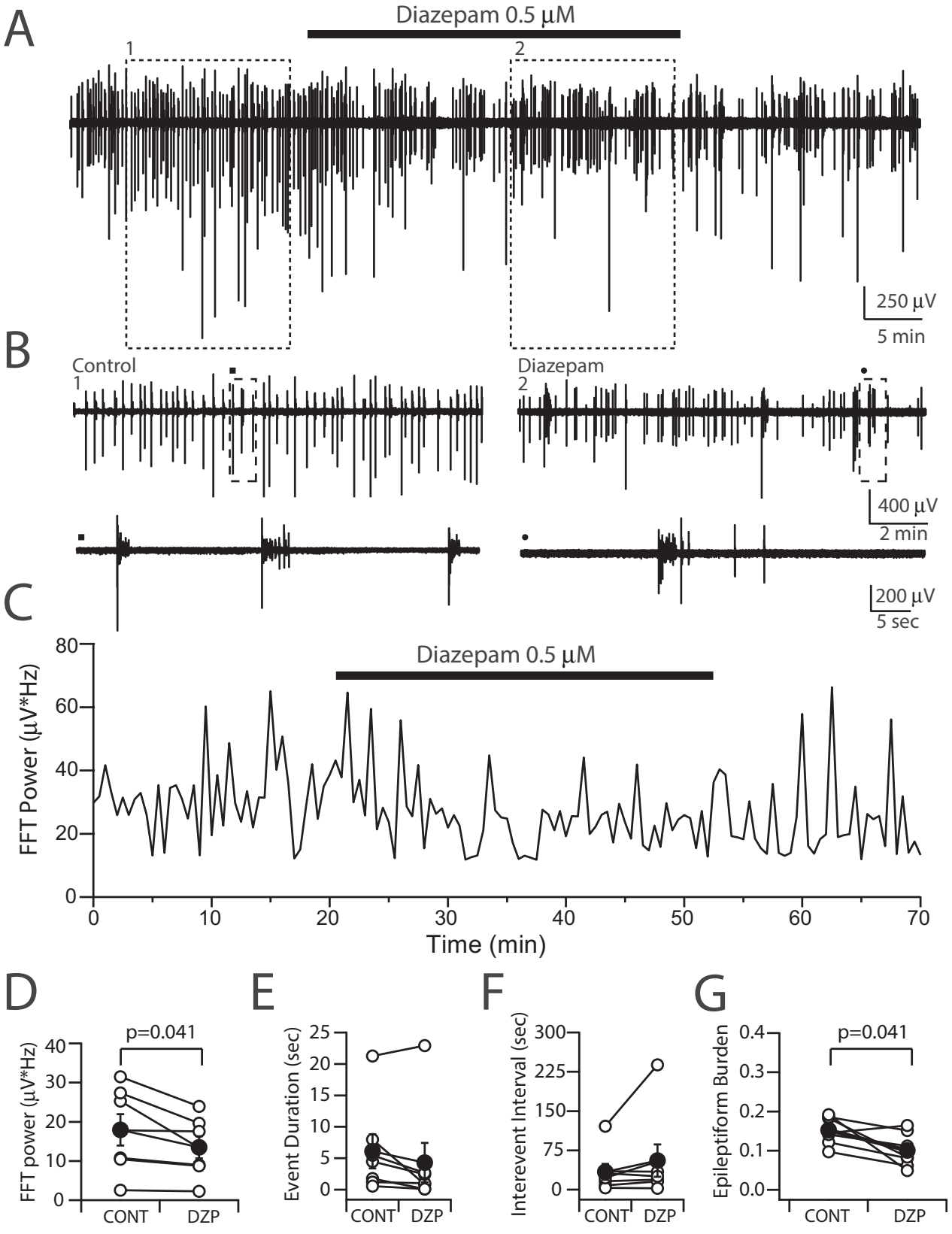


 

**Table 2.** Effect of diazepam at different ages in neocortical organotypic slices.

| | FFT power ($\mu V \times Hz$) | | Event duration (sec) | | Interevent interval (sec) | | Epileptiform burden ratio | | |
|---|---|---|---|---|---|---|---|---|---|
| | CONT | DZP | CONT | DZP | CONT | DZP | CONT | DZP | *n* |
| DIV5–6 | 12.3 ± 1.5 | 10.8 ± 1.3 | 4.82 ± 4.48 | 6.72 ± 4.19 | 117.6 ± 70.1 | 258.8 ± 185.6 | 0.05 ± 0.01 | 0.07 ± 0.04 | 6 |
| DIV9–10 | 18.0 ± 4.0 | 13.5 ± 2.8 | 6.10 ± 2.71 | 4.30 ± 3.13 | 33.9 ± 15.1 | 55.5 ± 31.0 | 0.15 ± 0.01 | 0.10 ± 0.02 | 7 |
| DIV15–16 | 23.4 ± 2.8 | 12.9 ± 1.0 | 1.01 ± 0.32 | 0.48 ± 0.21 | 4.99 ± 0.93 | 10.4 ± 4.10 | 0.22 ± 0.03 | 0.09 ± 0.03 | 6 |

Mean ± SEM. See text for statistical significance. FFT, Fast Fourier Transform; CONT, control; DZP, diazepam; DIV, days in vitro.

has been described in the hippocampal model.[37,38] It is unclear why these models have spontaneous seizures yet it seems to be related to intrinsic alterations in the cellular or network properties of organotypic slices,[38,62] and not related to ictal cell death or the prevention of ictal and interictal activity.[37] The occurrence of spontaneous epileptiform activity can allow the study of epileptogenesis without relying on application of acute convulsant conditions that might compromise the efficacy of anticonvulsants, for example methods that alter ionic compositions[63] including the Low $Mg^{2+}$ model,[41,42] high $K^+$ model,[43,44] blocking $K^+$ channels with 4-aminopyridine,[45,46] or activating kainate receptors.[47] Unfortunately, up to date, we have not been able to grow organotypic slices directly from adult animals to study seizure activity starting in the adult age, or with sufficient thalamo-cortical connections.

The definition of seizures in vitro is a contentious one.[54–56] If we take a conservative definition of events lasting more than 10 sec,[55,56] of the three ages tested, DIV15–16 had less seizure-like activity compared to earlier ages. At these older ages, the epileptiform activity was short, frequent, and regular, and thus more reminiscent of the EEG pattern termed Periodic Lateralized Epileptiform Discharges (PLEDs) than interictal spikes. The regularity and frequency of the discharges support the comparison to PLEDs.[64–66] The original description included the speculation that PLEDs develop as a consequence of disconnection from subcortical structures such as the thalamus.[64] Our neocortical preparation is similarly disconnected and thus strongly supports this idea. It remains unknown why older slices with a low $[Cl^-]_i$ have persistent spontaneous epileptiform activity with a high epileptiform activity burden. Circuit reorganization leading to hyper-synchrony may be a plausible explanation[62] while the low neuronal $[Cl^-]_i$ may prevent interictal activity into progressing to a full ictal event.

$[Cl^-]_i$ decreases during early development.[5] This has been shown in multiple brain areas including the neocortex,[2,4,6,51,67] hippocampus,[8,68,69] spinal cord,[70] hypothalamic neurons,[71] and other structures. We showed that in neocortical organotypic slices at DIV5–6, more than 75% of neurons have $[Cl^-]_i$ above 20 mM compared to around 7% at DIV9–10 and DIV15. A higher $[Cl^-]_i$ has been associated with cutting trauma in brain slices,[52] but as shown in Figure 1F, the high $[Cl^-]_i$ in younger slices extends throughout all depths of the slice and therefore cannot be attributed to trauma. Also, neurons traumatized during acute slice preparation die in the first days of culture.[37] Our current $[Cl^-]_i$ data are in agreement with a similar decrease in $[Cl^-]_i$ seen during early development in the acute thalamo-cortical slices.[6] In this preparation, the $[Cl^-]_i$ in thalamic neurons was always lower than the $[Cl^-]_i$ of neocortical neurons yet both had slicing trauma.[6] Therefore, these new data in conjunction with the acute slice data in the neocortex[6] argue that while acute trauma can lead to very high $[Cl^-]_i$ in the most superficial neurons, the majority of neurons during early development have elevated $[Cl^-]_i$ independent of trauma. Future in vivo $[Cl^-]_i$ measurements will allow us to clarify the role of development versus trauma.

The progressive decrease in $[Cl^-]_i$ over time has been associated in the past with a change in the expression of different CCCs.[5,10,13,72] However, there are brain areas where CCC expression does not correlate with changes in $[Cl^-]_i$[21,73–75] and the CCCs can transport $Cl^-$ in either

**Figure 5.** Diazepam is effective in decreasing epileptiform activity at DIV15 neocortical organotypic slices. (A) Extracellular recording of epileptiform activity recorded in regular aCSF from layer II/III of a DIV15 organotypic neocortical slice. Diazepam perfusion indicated with black line. (B) *Upper panels:* Higher magnification of characteristic events from dashed boxes in (A). Control condition (1), diazepam condition (2). *Lower panels:* higher magnifications of events in dashed boxes from upper panels. Control condition (■), diazepam condition (●). (C) FFT power calculated every 30 sec from the trace in (A). (D) FFT power was statistically different between paired control (CONT) and diazepam (DZP) conditions. (E) Event duration was statistically different between paired conditions. (F) Interevent interval between both paired conditions. (G) Epileptiform burden was statistically different between paired conditions. Dark circles are mean ± SEM; $n = 6$; paired *t*-test. DIV, days in vitro; FFT, Fast Fourier Transform.

 

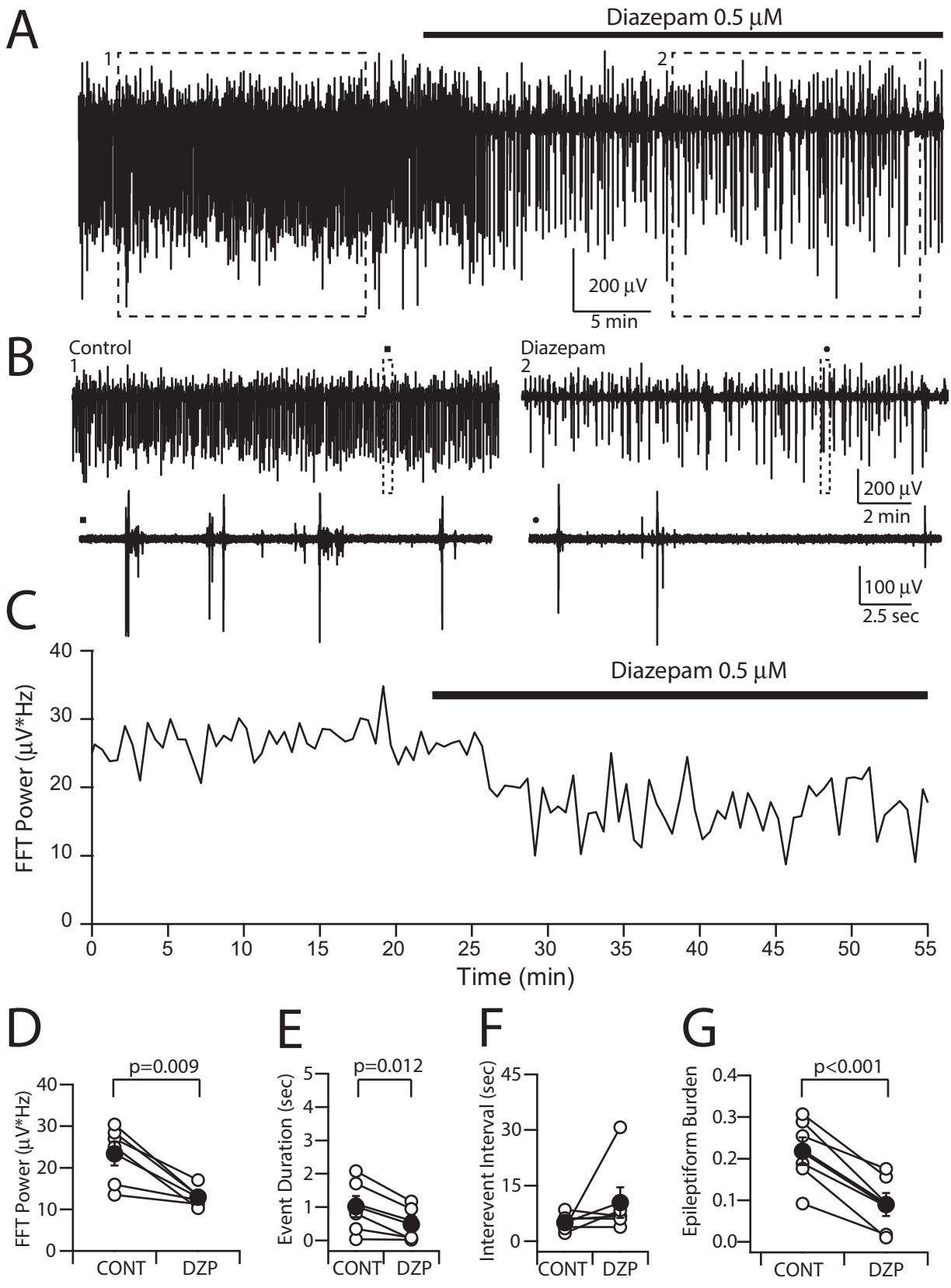


 

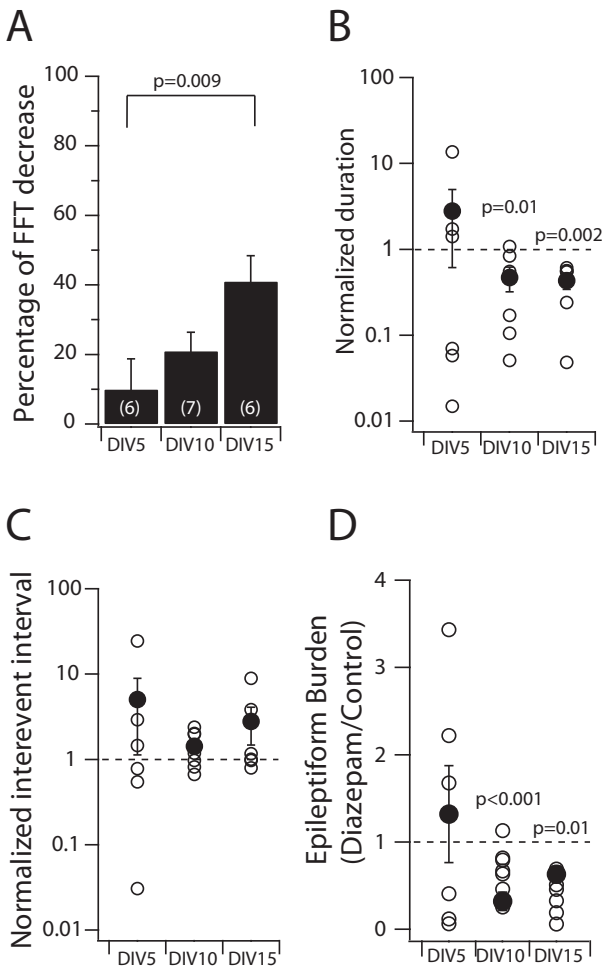


**Figure 6.** Effect of diazepam at different ages in neocortical organotypic slices. (A) Percentage of FFT power decrease at different DIV ages (DIV5 represents DIV5–6; DIV10 represents DIV9–10). Number of slices in parenthesis. (B) Normalized event duration of diazepam effect (diazepam/control). (C) Normalized interevent interval of diazepam effect. (D) Normalized epileptiform burden of diazepam effect. *P* above circles indicate one sample *t*-test values. Mean ± SEM. FFT, Fast Fourier Transform; DIV, days in vitro.

direction[19,76–78] depending on the free-energy gradients for the transported species. A more plausible explanation (and energetically favorable) for the developmental decrease in $[Cl^-]_i$ is that the immobile anions inside and outside neurons that set $[Cl^-]_i$ increase during development.[19,20] The transporters are more likely involved in compensating the movement of $Cl^-$ during fast synaptic transmission in order to reset $E_{Cl}$ and water flux.[20,75,77]

If CCCs do not determine $[Cl^-]_i$, and CCCs help restore equilibrium after synaptic activity, why should neonatal seizures be treated with antagonists of these CCCs?[6,7,79,80] The vast majority of neonatal seizures occur in the setting of brain injury.[81] In this setting, $[Cl^-]_i$ increases in a CCC-dependent manner,[52] which exacerbates the high population mean $[Cl^-]_i$ in immature neural networks, and facilitates GABAergic inhibitory failure and seizures. Furthermore, the efficacy of other anticonvulsants may be affected when GABA signaling is compromised. Drugs that decrease $[Cl^-]_i$ by blocking NKCC1 (e.g., bumetanide) could give us an extra level of confidence when using benzodiazepines or phenobarbital at this age. While a recent clinical trial with no control group showed that bumetanide, as an add on medication, did not improve seizure outcome in a population of human neonates with seizures associated with hypoxic-ischemic encephalopathy,[82] this is largely because four of the nine neonates had no seizures during the predrug baseline. It is of note that five of the nine neonates with baseline seizures had more than 80% reduction of seizure burden.[83] Another study is currently ongoing studying pharmacokinetic and safety data of bumetanide in another population of human neonates with seizures (NCT00830531). Its results can help determine if other drugs that alter $Cl^-$ need to be studied.

We have found a lack of anticonvulsant efficacy in the neocortex by a clinically relevant dose of diazepam at DIV5–6. This is comparable to the effect seen by phenobarbital in the acute slices at P9–10 in the Low-$Mg^{2+}$ and 4-AP models.[6] In fact, in 50% of the neocortical organotypic slices the epileptiform activity increased with diazepam. This observation could explain the paradoxical effect of inducing seizures, myoclonus and/or abnormal movements in some human neonates when benzodiazepines are given.[32–36] As $[Cl^-]_i$ decreases during development, diazepam becomes more effective (100% of slices had a decrease in epileptiform activity at DIV15). How can it be that during early development, diazepam can either enhance or decrease epileptiform activity in different slices of the same age? GABA can be excitatory or inhibitory dependent on the relation of $E_{GABA}$ to the neuron's RMP. As we and others have demonstrated,[3,6,19,84] the interneuronal $[Cl^-]_i$ is variable, and more so at earlier ages. Therefore, the net circuit effect of GABA and its allosteric modulators is not only dependant on one neuron's $[Cl^-]_i$ but on the proportion of neurons with elevated and low $[Cl^-]_i$ and their role in synchrony. In our case, at DIV5–6 more than 75% of neurons have $[Cl^-]_i$ above 20 mM compared to around 7% at DIV9–10 and DIV15. Furthermore, a higher $[Cl^-]_i$ in a small proportion of interneurons, who are able to synchronize short and long distant networks[85–87] could have more proconvulsive actions compared to higher $[Cl^-]_i$ in principal cells. In addition, the relation between high $[Cl^-]_i$ neurons, $GABA_AR$ subunit expression switch during development and pathology needs to taken in consideration.[88,89]

By using multiple methods for quantification of epileptiform activity, we show that measurements that take into

 

account two or more event characteristics, in our case epileptiform activity burden (duty cycle) and FFT power, are more sensitive in discriminating drug effects than a single parameter characterization. This is reminiscing of the *Imean* method to measure $GABA_AR$ currents.[90]

In conclusion, diazepam is more efficacious as an anticonvulsive medication at older developmental ages and its anticonvulsant effect is correlated with neuronal $[Cl^-]_i$. Furthermore, our study reveals why some human neonates show a paradoxical effect to benzodiazepines, and should make us aware of this possible effect when benzodiazepines are given.

## Acknowledgments

Michelle Mail provided technical support in the preparation of the organotypic slices. J. G. was supported by the American Academy of Neurology/the American Brain Foundation/Beyond Batten Disease Foundation Fellowship. K. S. was supported by R01NS74772-04 and 5R01NS40109-14.

## Author Contributions

J. G. designed and performed the experiments, analyzed the data, and wrote the manuscript. K. S. designed experiments and edited the manuscript.

## Conflict of Interest

None declared.

### References

1. Bormann J, Hamill O, Sakmann B. Mechanism of anion permeation through channels gated by glycine and gamma-aminobutyric acid in mouse cultured spinal neurones. J Physiol 1987;385:243–286.
2. Owens DF, Boyce LH, Davis MB, Kriegstein AR. Excitatory GABA responses in embryonic and neonatal cortical slices demonstrated by gramicidin perforated-patch recordings and calcium imaging. J Neurosci 1996;16:6414–6423.
3. Yuste R, Katz LC. Control of postsynaptic $Ca^{2+}$ influx in developing neocortex by excitatory and inhibitory neurotransmitters. Neuron 1991;6:333–344.
4. Luhmann HJ, Prince DA. Postnatal maturation of the GABAergic system in rat neocortex. J Neurophysiol 1991;65:247–263.
5. Ben-Ari Y, Gaiarsa J-L, Tyzio R, Khazipov R. GABA: a pioneer transmitter that excites immature neurons and generates primitive oscillations. Physiol Rev 2007;87:1215–1284.
6. Glykys J, Dzhala VI, Kuchibhotla KV, et al. Differences in cortical versus subcortical GABAergic signaling: a candidate mechanism of electroclinical uncoupling of neonatal seizures. Neuron 2009;63:657–672.
7. Dzhala VI, Talos DM, Sdrulla DA, et al. NKCC1 transporter facilitates seizures in the developing brain. Nat Med 2005;11:1205–1213.
8. Valeeva G, Valiullina F, Khazipov R. Excitatory actions of GABA in the intact neonatal rodent hippocampus in vitro. Front Cell Neurosci 2013;7:20.
9. Cancedda L, Fiumelli H, Chen K, Poo M. Excitatory GABA action is essential for morphological maturation of cortical neurons in vivo. J Neurosci 2007;27:5224–5235.
10. Yamada J, Okabe A, Toyoda H, et al. $Cl^-$ uptake promoting depolarizing GABA actions in immature rat neocortical neurones is mediated by NKCC1. J Physiol 2004;557(Pt 3):829–841.
11. Stein V, Hermans-Borgmeyer I, Jentsch TJ, Hübner CA. Expression of the KCl cotransporter KCC2 parallels neuronal maturation and the emergence of low intracellular chloride. J Comp Neurol 2004;468:57–64.
12. Ben-Ari Y. Excitatory actions of GABA during development: the nature of the nurture. Nat Rev Neurosci 2002;3:728–739.
13. Kahle KT, Staley KJ, Nahed BV, et al. Roles of the cation-chloride cotransporters in neurological disease. Nat Clin Pract Neurol 2008;4:490–503.
14. Plotkin MD, Snyder EY, Hebert SC, Delpire E. Expression of the Na-K-2Cl cotransporter is developmentally regulated in postnatal rat brains: a possible mechanism underlying GABA's excitatory role in immature brain. J Neurobiol 1997;33:781–795.
15. Baker NA, Sept D, Joseph S, et al. Electrostatics of nanosystems: application to microtubules and the ribosome. Proc Natl Acad Sci USA 2001;98:10037–10041.
16. Tang JX, Janmey PA. The polyelectrolyte nature of F-actin and the mechanism of actin bundle formation. J Biol Chem 1996;271:8556–8563.
17. Poulain FE, Sobel A. The microtubule network and neuronal morphogenesis: dynamic and coordinated orchestration through multiple players. Mol Cell Neurosci 2010;43:15–32.
18. Dent EW, Merriam EB, Hu X. The dynamic cytoskeleton: backbone of dendritic spine plasticity. Curr Opin Neurobiol 2011;21:175–181.
19. Glykys J, Dzhala V, Egawa K, et al. Local impermeant anions establish the neuronal chloride concentration. Science 2014;343:670–675.
20. Delpire E, Staley KJ. Novel determinants of the neuronal $Cl^-$ concentration. J Physiol 2014;592(Pt 19):4099–4114.
21. Nickell WT, Kleene NK, Gesteland RC, Kleene SJ. Neuronal chloride accumulation in olfactory epithelium of mice lacking NKCC1. J Neurophysiol 2006;95:2003–2006.
22. Doyon N, Prescott SA, Castonguay A, et al. Efficacy of synaptic inhibition depends on multiple, dynamically

 

interacting mechanisms implicated in chloride homeostasis. PLoS Comput Biol 2011;7:e1002149.
23. Pressler RM, Mangum B. Newly emerging therapies for neonatal seizures. Semin Fetal Neonatal Med 2013;18:216–223.
24. Rennie JM, Boylan GB. Neonatal seizures and their treatment. Curr Opin Neurol 2003;16:177–181.
25. Connell J, Oozeer R, de Vries L, et al. Clinical and EEG response to anticonvulsants in neonatal seizures. Arch Dis Child 1989;64:459–464.
26. Painter MJ, Scher MS, Stein AD, et al. Phenobarbital compared with phenytoin for the treatment of neonatal seizures. N Engl J Med 1999;341:485–489.
27. Van Rooij LGM, Hellström-Westas L, de Vries LS. Treatment of neonatal seizures. Semin Fetal Neonatal Med 2013;18:209–215.
28. Mcgoldrick MK, Galanopoulou AS. Developmental pharmacology of benzodiazepines under normal and pathological conditions. Epileptic Disord 2014;16:S59–S68.
29. Boylan GB, Rennie JM, Chorley G, et al. Second-line anticonvulsant treatment of neonatal seizures: a video-EEG monitoring study. Neurology 2004;62:486–488.
30. Shany E, Benzaqen O, Watemberg N. Comparison of continuous drip of midazolam or lidocaine in the treatment of intractable neonatal seizures. J Child Neurol 2007;22:255–259.
31. Sheth RD, Buckley DJ, Gutierrez AR, et al. Midazolam in the treatment of refractory neonatal seizures. Clin Neuropharmacol 1996;19:165–170.
32. Ng E, Klinger G, Shah V, et al. Safety of benzodiazepines in newborns. Ann Pharmacother 2002;36:1150–1155.
33. Chess PR, D'Angio CT. Clonic movements following lorazepam administration in full-term infants. Arch Pediatr Adolesc Med 1998;152:98–99.
34. Sexson WR, Thigpen J, Stajich GV. Stereotypic movements after lorazepam administration in premature neonates: a series and review of the literature. J Perinatol 1995;15:146–149; quiz 150–1.
35. Waisman D, Weintraub Z, Rotschild A, Bental Y. Myoclonic movements in very low birth weight premature infants associated with midazolam intravenous bolus administration. Pediatrics 1999;104(3 Pt 1):579.
36. Lee DS, Wong HA, Knoppert DC. Myoclonus associated with lorazepam therapy in very-low-birth-weight infants. Biol Neonate 1994;66:311–315.
37. Berdichevsky Y, Dzhala V, Mail M, Staley KJ. Interictal spikes, seizures and ictal cell death are not necessary for post-traumatic epileptogenesis in vitro. Neurobiol Dis 2012;45:774–785.
38. Dyhrfjeld-Johnsen J, Berdichevsky Y, Swiercz W, et al. Interictal spikes precede ictal discharges in an organotypic hippocampal slice culture model of epileptogenesis. J Clin Neurophysiol 2010;27:418–424.
39. Dzhala V, Staley KJ. Acute and chronic efficacy of bumetanide in an in vitro model of posttraumatic epileptogenesis. CNS Neurosci Ther 2015;21:173–180.
40. McBain CJ, Boden P, Hill RG. Rat hippocampal slices "in vitro" display spontaneous epileptiform activity following long-term organotypic culture. J Neurosci Methods 1989;27:35–49.
41. Mody I, Lambert JD, Heinemann U. Low extracellular magnesium induces epileptiform activity and spreading depression in rat hippocampal slices. J Neurophysiol 1987;57:869–888.
42. Schuchmann S, Buchheim K, Meierkord H, Heinemann U. A relative energy failure is associated with low-$Mg^{2+}$ but not with 4-aminopyridine induced seizure-like events in entorhinal cortex. J Neurophysiol 1999;81:399–403.
43. Traynelis SF, Dingledine R. Potassium-induced spontaneous electrographic seizures in the rat hippocampal slice. J Neurophysiol 1988;59:259–276.
44. Jensen MS, Yaari Y. Role of intrinsic burst firing, potassium accumulation, and electrical coupling in the elevated potassium model of hippocampal epilepsy. J Neurophysiol 1997;77:1224–1233.
45. Avoli M, Psarropoulou C, Tancredi V, Fueta Y. On the synchronous activity induced by 4-aminopyridine in the CA3 subfield of juvenile rat hippocampus. J Neurophysiol 1993;70:1018–1029.
46. Dzhala VI, Staley KJ. Transition from interictal to ictal activity in limbic networks in vitro. J Neurosci 2003;23:7873–7880.
47. Khalilov I, Holmes GL, Ben-Ari Y. In vitro formation of a secondary epileptogenic mirror focus by interhippocampal propagation of seizures. Nat Neurosci 2003;6:1079–1085.
48. Cowan F, Rutherford M, Groenendaal F, et al. Origin and timing of brain lesions in term infants with neonatal encephalopathy. Lancet 2003;361:736–742.
49. Kuner T, Augustine GJ. A genetically encoded ratiometric indicator for chloride: capturing chloride transients in cultured hippocampal neurons. Neuron 2000;27:447–459.
50. Gähwiler BH, Capogna M, Debanne D, et al. Organotypic slice sultures: a technique has come of age. Trends Neurosci 1997;20:471–477.
51. Rheims S, Minlebaev M, Ivanov A, et al. Excitatory GABA in rodent developing neocortex in vitro. J Neurophysiol 2008;100:609–619.
52. Dzhala V, Valeeva G, Glykys J, et al. Traumatic alterations in GABA signaling disrupt hippocampal network activity in the developing brain. J Neurosci 2012;32:4017–4031.
53. Lillis KP, Kramer MA, Mertz J, et al. Pyramidal cells accumulate chloride at seizure onset. Neurobiol Dis 2012;47:358–366.

 

54. D'Ambrosio R, Hakimian S, Stewart T, et al. Functional definition of seizure provides new insight into post-traumatic epileptogenesis. Brain 2009;132:2805–2821.
55. White AM, Williams PA, Ferraro DJ, et al. Efficient unsupervised algorithms for the detection of seizures in continuous EEG recordings from rats after brain injury. J Neurosci Methods 2006;152:255–266.
56. White A, Williams PA, Hellier JL, et al. EEG spike activity precedes epilepsy after kainate-induced status epilepticus. Epilepsia 2010;51:371–383.
57. Study RE, Barker JL. Diazepam and (–)-pentobarbital: fluctuation analysis reveals different mechanisms for potentiation of gamma-aminobutyric acid responses in cultured central neurons. Proc Natl Acad Sci USA 1981;78:7180–7184.
58. Macdonald R, Barker JL. Benzodiazepines specifically modulate GABA-mediated postsynaptic inhibition in cultured mammalian neurones. Nature 1978;271:563–564.
59. Choi D, Farb D, Fischbach G. Chlordiazepoxide selectively augments GABA action in spinal cord cell cultures. Nature 1977;269:342–344.
60. Anderson G, Miller J. Benzodiazepines. Chemistry, Biotransformation and Pharmacokinetics. In: Levy R, Meldrum B, Mattson R, Perucca E, eds. Antiepileptic drugs: 5th edn. Philadelphia: Lippincott Williams & Wilkins; 2002. 187–205.
61. Greenblatt DJ, Sethy VH. Benzodiazepine concentrations in brain directly reflect receptor occupancy: studies of diazepam, lorazepam, and oxazepam. Psychopharmacology 1990;102:373–378.
62. Lillis KP, Wang Z, Mail M, et al. Evolution of network synchronization during early epileptogenesis parallels synaptic circuit alterations. J Neurosci 2015;35:9920–9934.
63. Coppola A, Moshé SL. Animal models. Handb Clin Neurol 2012;107:63–98.
64. Cobb W, Hill D. Electroencephalogram in subacute progressive encephalitis. Brain 1950;73:392–404.
65. Chatrian G, Shaw C, Leffman H. The significance of periodic lateralized epileptiform discharges in EEG: an electrographic, clinical and pathological study. Electroencephalogr Clin Neurophysiol 1964;17:177–193.
66. Andraus MEC, Andraus CF, Alves-Leon SV. Periodic EEG patterns: importance of their recognition and clinical significance. Arq Neuropsiquiatr 2012;70:145–151.
67. LoTurco JJ, Owens DF, Heath MJS, et al. GABA and glutamate depolarize cortical progenitor cells and inhibit DNA synthesis. Neuron 1995;15:1287–1298.
68. Tyzio R, Holmes GL, Ben-Ari Y, Khazipov R. Timing of the developmental switch in GABA(A) mediated signaling from excitation to inhibition in CA3 rat hippocampus using gramicidin perforated patch and extracellular recordings. Epilepsia 2007;48(Suppl 5):96–105.
69. Dzhala VI, Staley KJ. Excitatory actions of endogenously released GABA contribute to initiation of ictal epileptiform activity in the developing hippocampus. J Neurosci 2003;23:1840–1846.
70. Obata K, Oide M, Tanaka H. Excitatory and inhibitory actions of GABA and glycine on embryonic chick spinal neurons in culture. Brain Res 1978;144:179–184.
71. Chen G, Trombley PQ, van den Pol AN. Excitatory actions of GABA in developing rat hypothalamic neurones. J Physiol 1996;494(Pt 2):451–464.
72. Payne JA. Molecular operation of the cation chloride cotransporters: ion binding and inhibitor interaction. Curr Top Membr 2012;70:215–237.
73. Balakrishnan V, Becker M, Löhrke S, et al. Expression and function of chloride transporters during development of inhibitory neurotransmission in the auditory brainstem. J Neurosci 2003;23:4134–4145.
74. Mao S, Garzon-Muvdi T, Di Fulvio M, et al. Molecular and functional expression of cation-chloride cotransporters in dorsal root ganglion neurons during postnatal maturation. J Neurophysiol 2012;108:834–852.
75. Zhu L, Lovinger D, Delpire E. Cortical neurons lacking KCC2 expression show impaired regulation of intracellular chloride. J Neurophysiol 2005;93:1557–1568.
76. DeFazio R, Keros S, Quick MW, Hablitz JJ. Potassium-coupled chloride cotransport controls intracellular chloride in rat neocortical pyramidal neurons. J Neurosci 2000;20:8069–8076.
77. Brumback AC, Staley KJ. Thermodynamic regulation of NKCC1-mediated $Cl^-$ cotransport underlies plasticity of GABA(A) signaling in neonatal neurons. J Neurosci 2008;28:1301–1312.
78. Payne JA. Functional characterization of the neuronal-specific K-Cl cotransporter: implications for [K+]o regulation. Am J Physiol Cell Physiol 1997;273:1516–1525.
79. Liu Y, Shangguan Y, Barks JDE, Silverstein FS. Bumetanide augments the neuroprotective efficacy of phenobarbital plus hypothermia in a neonatal hypoxia–ischemia model. Pediatr Res 2012;71:559–565.
80. Dzhala VI, Brumback AC, Staley KJ. Bumetanide enhances phenobarbital efficacy in a neonatal seizure model. Ann Neurol 2008;63:222–235.
81. Vasudevan C, Levene M. Epidemiology and aetiology of neonatal seizures. Semin Fetal Neonatal Med 2013;18:185–191.
82. Pressler RM, Boylan GB, Marlow N, et al. Bumetanide for the treatment of seizures in newborn babies with hypoxic ischaemic encephalopathy (NEMO): an open-label, dose finding, and feasibility phase 1/2 trial. Lancet Neurol 2015;4422:1–9.
83. Thoresen M, Sabir H. Epilepsy: neonatal seizures still lack safe and effective treatment. Nat Rev Neurol 2015;11:311–312.
84. Ebihara S, Shirato K, Harata N, Akaike N. Gramicidin-perforated patch recording: GABA response in mammalian

 

neurones with intact intracellular chloride. J Physiol 1995;484(Pt 1):77–86.
85. Cobb SR, Buhl EH, Halasy K, et al. Synchronization of neuronal activity in hippocampus by individual GABAergic interneurons. Nature 1995;378:75–78.
86. D'Antuono M, Louvel J, Köhling R, et al. GABA A receptor-dependent synchronization leads to ictogenesis in the human dysplastic cortex. Brain 2004;127:1626–1640.
87. Mann EO, Paulsen O. Role of GABAergic inhibition in hippocampal network oscillations. Trends Neurosci 2007;30:343–349.
88. Alfonsa H, Merricks EM, Codadu NK, et al. The contribution of raised intraneuronal chloride to epileptic network activity. J Neurosci 2015;35:7715–7726.
89. Laurie DJ, Wisden W, Seeburg PH. The distribution of thirteen GABAA receptor subunit mRNAs in the rat brain. III. Embryonic and postnatal development. J Neurosci 1992;12:4151–4172.
90. Glykys J, Mody I. The main source of ambient GABA responsible for tonic inhibition in the mouse hippocampus. J Physiol 2007;582(Pt 3):1163–1178.

 